STUDY OF WATER ABSORPTION LINES IN THE NEAR INFRARED

Ali Javan

Massachusetts Institute of Technology

Prepared for:

Advanced Research Projects Agency

17 February 1975

The views and conclusions contained in this document are those of the authors and should not be interpreted as necessarily representing the official policies, either expressed or implied, of the Advanced Research Projects Agency or the U. S. Government.

MIL-STD-847A
31 January 1973

Unclassified

SECURITY CLASSIFICATION OF THIS PAGE (When Data Entered)

REPORT DOCUMENTATION PAGE	READ INSTRUCTIONS BEFORE COMPLETING FORM
1. REPORT NUMBER: Semi-Annual Technical Reports #2-3	2. GOVT ACCESSION NO. / 3. RECIPIENT'S CATALOG NUMBER: AD/A-005636
4. TITLE (and Subtitle): STUDY OF WATER ABSORPTION LINES IN THE NEAR INFRARED	5. TYPE OF REPORT & PERIOD COVERED: Scientific Interim
	6. PERFORMING ORG. REPORT NUMBER: Semi-Annual Tech. Report #2 - #3
7. AUTHOR(s): Ali Javan	8. CONTRACT OR GRANT NUMBER(s): N000-14-75-C-0306
9. PERFORMING ORGANIZATION NAME AND ADDRESS: Department of Physics Massachusetts Institute of Tech. Cambridge, Mass. 02139	10. PROGRAM ELEMENT, PROJECT, TASK AREA & WORK UNIT NUMBERS: ARPA order 1807 Program Code #5E20
11. CONTROLLING OFFICE NAME AND ADDRESS: NAVAL RESEARCH LABS. OPTICAL SCIENCE DIVISION CODE 6504 WASHINGTON, D.C.	12. REPORT DATE: Feb. 17, 1975
	13. NUMBER OF PAGES
14. MONITORING AGENCY NAME & ADDRESS (if different from Controlling Office): Contract Monitor: John Walsh	15. SECURITY CLASS. (of this report): Unclassified
	15a. DECLASSIFICATION/DOWNGRADING SCHEDULE
16. DISTRIBUTION STATEMENT (of this Report)	
17. DISTRIBUTION STATEMENT (of the abstract entered in Block 20, if different from Report)	
18. SUPPLEMENTARY NOTES: This research was supported by the Advanced Research Project Agency of the Department of Defense ARPA order 1807.	
19. KEY WORDS (Continue on reverse side if necessary and identify by block number): Wings of Water Vapor Lines, Acoustical Modulator-Frequency Tuning. Velocity Dependent Collision Processes NH_3. Collision Induced Absorption in Rare Gas Mixture.	

20. ABSTRACT (Continue on reverse side if necessary and identify by block number)

Progress has been made in the following area:

1. Development of a Tunable 5 Micron Spin-Flip Raman Laser and Application to Precision Spectroscopy of H_2O.

DD FORM 1 JAN 73 1473 EDITION OF 1 NOV 65 IS OBSOLETE

Unclassified

CLASSIFICATION OF THIS PAGE (When Data Entered)

SECURITY CLASSIFICATION OF THIS PAGE (When Data Entered)

20. continued

2. Studies of Wings of Water Vapor Lines.

3. Other Spectroscopic Applications of the Spin-Flip Raman Laser.

4. Development of a Tunable 5 Micron Pulsed Laser.

5. Spectroscopy of D_2O Using an Acoustical Modulator for Frequency Tuning.

6. Velocity Dependence of Collision Processes in NH_3.

7. Theoretical Formulation of Absorption Far from Line Center - Collision Induced Absorption in Rare Gas Mixture.

SECURITY CLASSIFICATION OF THIS PAGE (When Data Entered)

TABLE OF CONTENTS

Introduction

This report summarizes progress of research sponsored by the Naval Research Laboratories, Contract No. N00014-75-C-0360 for the period November 1, 1973 through October 31, 1974. The goal of this program is to obtain the quantitative information necessary for a detailed understanding of the propagation behavior of intense laser radiation in the 2 to 5 micron region through a medium containing water vapor.

I. Development of a Tunable 5-μ Spin-flip Raman Laser and Application to Precision Spectroscopy of H_2O.

A gradient field permanent magnet spin-flip Raman (SFR) laser system which utilizes tapered pole pieces to give a field variation over the pole faces was used to measure the pressure broadening coefficients of the $\left[(000), 5_{15} \rightarrow (010), 6_{43}\right]$ transition of the ν_2 fundamental vibrational band in water vapor. We have also measured the absorption linewidth of the $\left[(000), 5_{32} \rightarrow (010), 6_{43}\right]$ transition in the atmosphere (22°c and 35% relative humidity) at a partial pressure of 7 torr.

Spin-flip Raman laser is composed of a 2-methylbutane cooled CO laser with a nominal output of 2 w, and a low carrier concentration Insb crystal, cooled below liquid helium temperature and placed between the pole faces of a permanent magnet. The SFR laser has both forward and backward outputs. The forward output was used to calibrate the frequency tuning of the SFR laser using a Fabry-Perot interferometer. This provides an independent frequency state accurate to within three percent. The backward output of the SFR laser was for the water vapor absorption spectroscopy. The permanent magnet could be positioned so that the first stokes line

of the SFR laser was near the water vapor absorption line and fine tuning was done electronically using Helmholtz coils mounted on the magnet. Since the tuning rate of low electron concentration (SFR) laser is high (~ 65 MH_z/G) a variation of only a few gauss is needed to sweep over a Doppler-limited absorption lineshape of water vapor. Further experimental details are discussed in Appendix III.

The results of collision broadening coefficients are found to be 44.6 ± 4 mhz/torr for nitrogen, 7.5 ± 0.7 mhz/torr for nitrogen, 5.7 ± 0.6 mhz/torr for oxygen, 2.9 ± 0.2 mhz/torr for Argon, and 2.75 mhz/torr for Xenon broadening. These coefficients were found to be in very good agreement with those calculated by Benedict and Kaplan[1,2] who used Anderson's theory to calculate the line width of H_2O - H_2O and H_2O - N_2 collisions. These results support the contention that the theory is valid for low-J transitions but is not accurate for high-J transitions[3], therefore, they can be helpful in the development of improved models of atmospheric absorption in the near infrared.

REFERENCES

1. W. S. Benedict, L. D. Kaplan, J. of Chemistry - Physics, 30, 388 (1959)
2. W. S. Benedict, L. D. Kaplan JQSRT 4 , 453 (1964).
3. F. A. Blum, K. W. Nill, P. L. Kelley, A. R. Cawala, and T. C. Harman, Science 177 , 694 (1972).

II. Studies of Wings of Water Vapor Lines

Having completed a set of measurements of lineshape features in the vicinity of water vapor resonances, preparations are now underway to explore the lineshape features at the wing of these absorption lines, particularly their deviation from Lorentzian behavior. For experimental convenience a novel balancing method is being planned in which the transmission at the wing of the line will be measured simultaneously with the transmission at the peak. The absorption coefficients at the wing will thus be given as ratios calibrated against the peak valves.

A tunable 5μm c.w. spin-flip Raman (SFR) laser will be used to probe the absorption line at various points, from line center up to a detuning of 1.2 cm^{-1}, the tuning range of the SFR laser. A fixed-frequency stable CO laser will be used as a reference to monitor the absorption on the wing, 2.7 cm^{-1} away from the peak. In order to enhance the absorption at the wings, we will broaden the line by adding nitrogen buffer gas. Some design considerations based on simple theoretical estimates are given below.

Our recent experiments, obtained values for nitrogen and self-broadening coefficients of water vapor resonances on several low J transitions which agreed closely with the theoretical predictions. For the present experiments we have chosen a line, $\left[(000), 5_{32} \longrightarrow (010), 6_{43}\right]$, which falls at 1889.58 cm^{-1}, for the fact that it is well isolated from other transitions. It follows from our earlier work that the theoretical values of 6.3 (nitrogen-broadening) and 31 (self-broadening) MHz/torr are reliable near line center. Measurements by Long et al[1] indicate that the absorption in the wings is considerably larger than that predicted

from a Lorentzian lineshape. Therefore, we can assume a Lorentzian behavior for the absorption line to obtain a lower limit for the absorption coefficient there.

The absorption coefficient can be written as:

$$\gamma = \frac{8\pi^2 |\mu_{ij}|^2 \nu}{3hc} Nf \left(1 - e^{-\frac{h\nu_0}{kT}}\right) \left[\frac{\frac{1}{2\pi\tau}}{(\nu-\nu_0)^2 + \left(\frac{1}{2\pi\tau}\right)^2}\right] \qquad (1)$$

where μ_{ij} is the matrix element of dipole transition, ν and ν_0 are the laser frequency and the center frequency of the transition, respectively, Nf is the density of molecules in the desired rotational-vibrational level, and $\frac{1}{2\pi\tau}$ is the half width at half height of the absorption line. If the line is broadened with nitrogen to the extent that the contribution of nitrogen broadening to the overall linewidth is much larger than that due to self broadening, then the absorption coefficient for the 1889.58 cm^{-1} line is given (in cm^{-1}) by

$$\gamma = \alpha \frac{3.2 \times 10^6 P_N P_{H_2O}}{(\nu-\nu_0)^2 + (3.2 \times 10^6 P_N)^2} \qquad (2)$$

where P_N and P_{H_2O}, the nitrogen and water vapor partial pressures are measured in Torr, and $\alpha = 2 \times 10^7$. The addition of nitrogen broadens the line in such a way that the absorption at the peak decreases while absorption at the wings increases. Therefore, the absorption coefficients at the peak and at the wings (2.7 cm^{-1} away from the peak will be

$$\gamma_{peak} = \alpha \frac{P_{H_2O}}{3.2 \times 10^6 P_N} \qquad (3)$$

$$\gamma_{wing} = \alpha \frac{3.2 \times 10^{6} P_N P_{H_2O}}{(\nu - \nu_0)^2} \qquad (4)$$

Since the absorption coefficient at the peak is much greater than that at the wing, we will use an experimental arrangement consisting of two cells, a short cell to probe the peak absorption and a long cell to probe the wing absorption, connected to a common reservoir (see figure 1). If we restrict ourselves to total pressures below 5 atmospheres, then a 2 meter long cell in conjunction with a cell of length 10 cm would have the same absorption. In this case the absorption in each cell will be about 15% at 5 atmospheres of N_2 and 7 torr of H_2O.

The experimental arrangement is shown in Figure 1. The CO and SFR lasers are balanced before they enter the cells, and the relative intensity is measured after they have passed through the cells. By detuning the SFR laser from the peak of the line, the absorption can be determined at several points along to the wing. The absorption magnitude can be obtained from the absolute value of the absorption at the peak.

In the experiments care will be taken to minimize the atmospheric absorption due to presence of water vapor in the air (~7 Torr). Amplitude fluctuation in the SFR laser resulting from tuning will be eliminated by taking the ratio of intensities measured before and after the cells. Finally by varying the buffer gas and H_2O partial pressures, we shall study the lineshape variations with pressure and lineshape curves can be obtained for various humidity conditions.

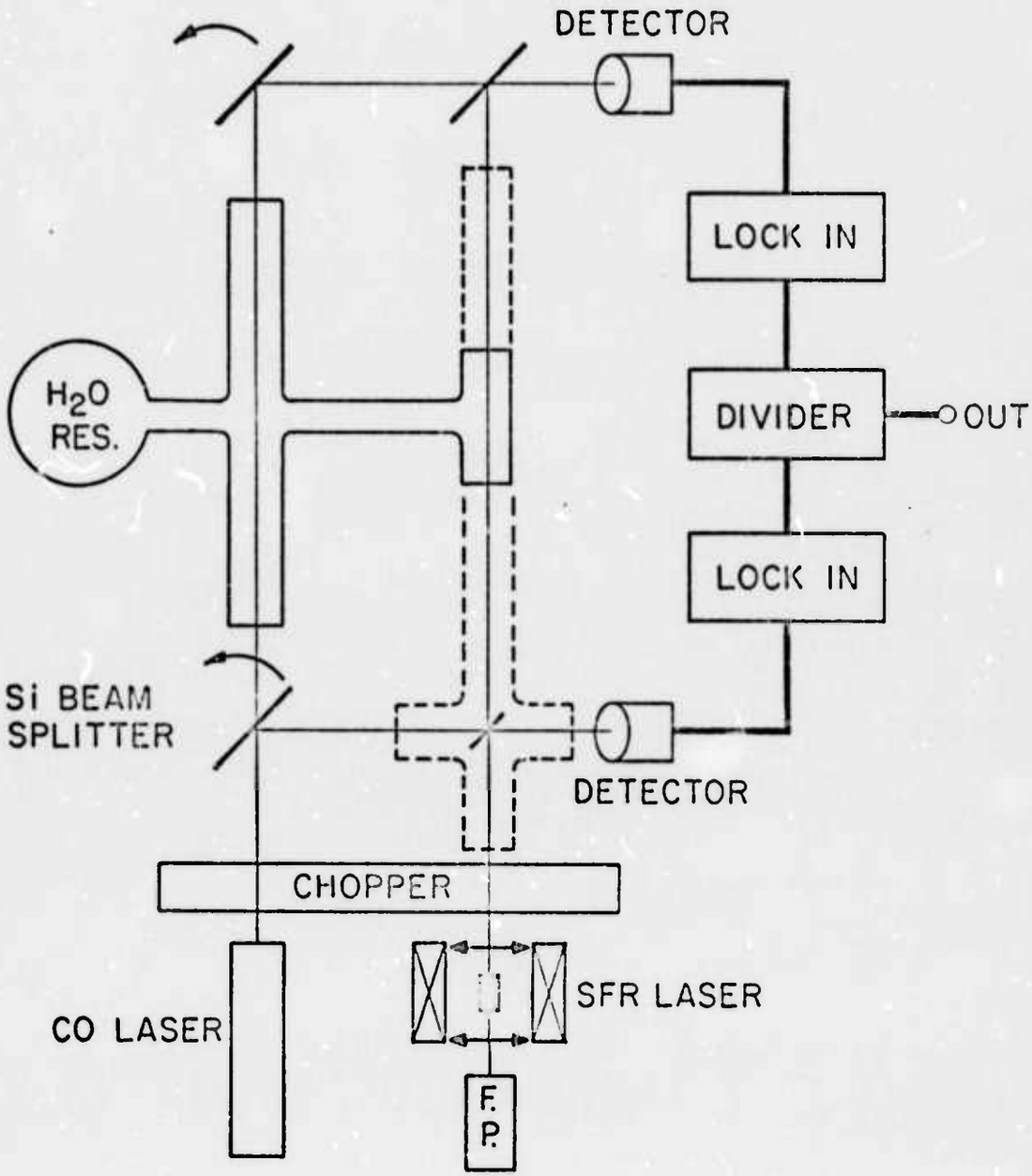
DETECTOR
LOCK IN
H_2O RES.
DIVIDER
OUT
LOCK IN
Si BEAM SPLITTER
DETECTOR
CHOPPER
CO LASER
SFR LASER
F. P.

6a

Figure 1

REFERENCES

1. R. K. Long, F. S. Mills, G. L. Trusty and D. F. Ford, presented at Autumn Meeting of Opt. Sec. Am. Oct. 1972

III. Other Spectroscopic Applications of Spin-flip Raman Lasers

An earlier version of the SFR laser described in App. 3 has been used in spectroscopy of NO.[1] This work was done primarily to test and evaluate the SFR laser. The spin-flip laser with its high output power and wide tuning range makes possible the study of many molecular systems which have transitions in the 5-6μ range. A long path White cell has been purchased and a high pressure absorption cell has been constructed to facilitate these studies.

Work has begun on using a proustite non-linear crystal to mix the spin-flip radiation with that of a CO laser and thus obtain tunable radiation at 2.5 μ. In a preliminary experiment, radiation from the CO pump laser itself was doubled. Experimental indications are that we can obtain several tenths of a microwatt of tunable cw power in this way.

REFERENCES

1. M. Guerra, S. Bruek, A. Mooradian, IEEE J. Quantum Electron. QE-9, 1157 (1973).

IV. Development of a Tunable 5 Micron Pulsed Laser

Design and construction of a 10-15 atmosphere pulsed CO_2 laser is now underway following completion of tests and studies on a similar device operated at 1-3 atmospheres. Preliminary results have been obtained at 5 atmospheres. At high pressures, CO_2 rotational transition lines overlap due to collision broadening allowing continuous tunability throughout the 10-μ region. The tunability of high pressure CO_2 lasers had already been demonstrated at 15 atmospheres using only a slightly different principle, and a CO_2 laser operating at 33 atmospheres has also been reported. An optical system, including a Smith cavity, is also being assembled for frequency tuning and mode selection of the high pressure laser oscillator. High-power pulses thus generated will be frequency doubled into the 5-μ region where it will be useful for saturation and pulse transmission studies of water vapor transition.

V. Spectroscopy of D_2O Using an Acoustical Modulator for Frequency Tuning

Absorption resonance in the ν_2 band of D_2O in near coincidence with CO_2 laser lines has been studied using acousto-optic modulation technique. The laser frequency is tuned by means of an acousto-optic modulator in order to give coincidence with the transition of the absorbing gas. The device consists of a quartz transducer bounded to the (111) face of a crystal of germainum. Ultrasonic waves of frequency W_s are set up in the crystal by the transducer, which then scatters part of the laser beam into a single wideband shifted from the laser center frequency by W_s. The sign of the shift is determined by choosing the appropriate angle between the acoutic wave and the light beam. Frequency shifts of up to ±500 MHz are possible, as compared with the ±40 MHz tunability of a regular CO_2 laser that uses a piezoelectric device to change the size of the laser cavity.

Coincidence between the R(22) line of the CO_2 laser and the $000,5_{33}$ - $010,4_{22}$ D_2O transition was obtained after shifting that line by 320 MHz. The center frequency value for this D_2O transition is then determined to be 1079.8628 ± .0002 cm^{-1}. This accurate value may be useful as a frequency calibration standard. Details of the experiment are presented in Appendix I.

VI. Velocity Dependence of Collision Processes in NH_3

A detailed study of the pressure broadening of an infrared transition in ammonia as a function of the velocity of the molecule has uncovered new spectroscopic features of this transition. The technique of using saturating and probe fields of different frequencies to investigate resonances for molecules having non-zero velocities along the fields' propagation direction was earlier applied to determine the velocity dependence of the collisions which contributed to the homogeneous widths of the resonances. In refining the technique to obtain data of sufficient accuracy to determine the intermolecular force laws, the hyperfine structure of the ν_2 as Q(8,7) transition in NH_3 was resolved. HFS components, weaker than the central resonance by a factor of 100, were brought out by strongly saturating the transition. The splitting of the components gives information about the structure of the molecule's excited state. A second feature observed in this study was the enhancement of the resonances when the gas molecules were subjected to a magnetic field. This is believed to be a manifestation of the stimulated Hanle effect and should provide a value for the g-factor of the excited state's magnetic moment. In addition to providing new spectroscopic information, these studies will facilitate the interpretation of the data on the velocity dependence of the collision cross sections.

VII. Theoretical Formulations of Absorption Far from Line Center

In order to develop a valid theory for the absorption far from line center which would be applicable to an understanding of the absorption in the wings of the water vapor lines, it is necessary to account for the absorption occuring during the collision. A program has been initiated to study collision induced absorption starting first with simple collision partners.

Calculations of the collision-induced absorption in a He-Ne mixture in the far infrared (200-600 cm^{-1}) have been published.[1] The present calculation includes an exact treatment of the collision dynamics and of the radiation field to the first order. The information used is the interatomic potential and dipole moment function. Using values of these parameters obtained from independent and extensive studies, we obtain values of the absorption coefficient which are about two orders of magnitude smaller than obtained previously. Possible causes of this large discrepancy are discussed.

Collision-induced absorption in He-Ar mixture has also been calculated. The calculation uses interaction atomic potential of R. Duren, R. Feltgen, W. Gaide, R. Helbing, and H. Pauly[2] to compute the wavefunction for relative translational motion. The absorption coefficient is computed for several dipole moment functions proposed in the literature. Best agreement with room temperature experimental results in the 67-200 cm^{-1} range is obtained if one uses a dipole moment which is the sum of Lacey-Byers Brown (L-BB)[3] short range contribution

and Whisnant-Byers Brown (W-BB) dispersion contribution.[4] Around 600 cm^{-1} at room temperature the absorption coefficient is better approximated by the sum of Matcha-Nesbet[5] short range contribution and W-BB dispersion contribution.

The contribution of the dispersion term to the absorption coefficient is much smaller than believed earlier by Levine. Appendix 2 discusses these calculations in more detail.

REFERENCES

1. R. D. Sharma and R. R. Hart, Chem. Phys. Letters 27, 589 (1974).
2. R. Duren, R. Feltgen, W. Gaide, R. Helbing, and H. Pauly, Phys Letters 18, 232 (1965)
3. A. J. Lacey and W. Byers Brown, Molecular Phys 27, 1013 (1974).
4. D. M. Whisnant and W. Byers Brown, Molecular Physics 26, 1105 (1973).
5. R. L. Matcha and R. K. Nesbet, Phys. Rev. 160, 72 (1967).
6. H. B. Levine, Phys. Rev. Letters, 21, 1512 (1968).

APPENDIX 1

OPTICAL PUMPING AND TUNABLE LASER SPECTROSCOPY OF THE ν_2 BAND OF D_2O

F. Keilmann, R.L. Sheffield, J.R.R. Leite, M.S. Feld and A. Javan

ABSTRACT

Absorption resonances in the ν_2 band of D_2O in near coincidence with CO_2 laser lines are reported and assigned. Optical pumping induces strong laser emission at new submillimeter wavelengths, confirming the assignments. Acousto-optic modulation is used to tune the R(22) line of the CO_2 laser into coincidence with the $000,5_{33}$-$010,4_{22}$ D_2O transition. Its center frequency is 1079.8628 cm^{-1}; the linewidth (HWHM) due to collisional broadening is 13 MHz/torr. D_2S and HDS transitions in near coincidence with CO_2 laser lines are also reported.

We have studied vibrational transitions in the ν_2 bands (the bending mode) of D_2O, HDS, and D_2S gases near 10μm[1]. These lie in the range of the $C^{12}O_2^{16}$ laser wavelengths. Absorption studies of the CO_2 laser lines showed tnat several molecular transitions were in near coincidence (within five to ten Doppler widths). Tentative assignment of these lines suggested that some of them could be optically pumped to produce far infrared radiation on branching transitions, and in subsequent experiments we obtained intense submillimeter emission at several wavelengths, confirming our assignments. Acousto-optically modulated CO_2 laser radiation was used as a tunable frequency source to tune to the center of one of the D_2O resonances, yielding an accurate value for the center frequency. The collision broadening coefficient and the dipole moment matrix element were also measured.

For the initial check of coincidences we used a low pressure continuous CO_2 laser which could be set by means of a grating to operate on any of about 70 lines extending from 9.2 to 10.8μm. The beam of roughly 1 W/cm^2 was sent through a 205 cm long absorption cell containing the gas under study. The transmitted power was measured with a thermopile. Up to about 15 torr (vapor pressure at room temperature) absorption of the CO_2 laser lines by D_2O yielded three near coincidences (Table I). In addition, one line each was found in D_2S and HDS. However, up to 100 torr no absorption was observed in H_2S.

Table II lists the observed D_2O transitions and their assignments.[2] The frequency separations between the CO_2 laser lines and the D_2O resonances were estimated from the measured

values of the CO_2 laser frequencies.[3] In addition to these close coincidences, several others were predicted from the tables to lie within $\sim$0.1 cm^{-1}. It has recently been shown[4] that it is possible to saturate molecular transitions detuned by many Doppler widths by means of an intense pump laser. On this basis we expected sizeable gain on coupled rotational transitions in the excited vibrational state by means of off-resonance optical pumping (Table II).

The experimental setup for optical pumping utilized a grating-controlled CO_2 laser delivering a few joules in approximately 150 nsec.[5] The linearly polarized laser beam, 3 cm in diameter, entered a 3 m long absorption cell through a NaCl window. The submillimeter laser emission built up essentially in a single pass and was transmitted through a TPX window. After passing through a double-mesh Fabry-Perot interferometer, the radiation reached an InSb detector sensitive to wavelengths from about 100 to 1000μm. In the experiments strong submillimeter emission (kW range) was found for five different pump lines at wavelengths between 100 and 400μm, as summarized in Table II. Laser oscillation occurred over a wide pressure range, from 15 torr (vapor pressure) down to about 0.02 torr, at roughly the same power level. At reduced pump power levels, however, oscillation could not be attained at the higher pressures. The emitted pulse followed the shape of the pump pulse at high pressures, whereas at lower pressures it lasted longer than the pump pulse, about 1μsec at 1.0 torr and 4μsec at 0.05 torr.

The observation of strong laser emission at the branching transitions confirms that sizeable saturation was achieved. The extent of saturation broadening is estimated to be about 3 GHz. In addition, the bandwidth of the high pressure pump laser is also 2-3 GHz.[5] Some expected branching transitions were not observed, suggesting that the detuning of the CO_2 laser lines from the pump transitions was larger than had been estimated using Ref. 2.

The submillimeter wavelengths were measured using the double-mesh interferometer (Table II). Due to low finesse and pulse-to-pulse variations in pump power, only the main spectral component could be resolved. Others, if present at 10% or less of the total power, would not have been seen. The accuracy of the measured wavelengths is $\pm$ 2 cm^{-1}. Theory[6] predicts that some of the submillimeter lines will be preferrentially polarized parallel to the pump laser field and others perpendicular to it, depending on the quantum numbers involved. The extent of polarization was measured using a wire grid polarizer. the 26 cm^{-1} line was found to be about 80% polarized; the other lines were polarized more than 95%. The observed relative polarization directions are listed in Table II.

Good agreement is found between the observed submillimeter wavelengths and those predicted using Ref. 2. Together with the measurements of relative polarization, this confirms our assignments. An unexplained exception is the transition pumped by the R(34) CO_2 line, which should be preferentially polarized perpendicular to the pump field according to the assignment

which fits the measured wavelengths.

The strong absorption of the $000,5_{33} - 010,4_{22}$ D_2O transition and its large variation in absorption over the tuning range of the probe laser indicated that the detuning of the molecular resonance from the CO_2 center frequency was small. In order to accurately determine the D_2O center frequency an acousto-optic modulator[7] was used to frequency shift the CO_2 laser lines. The device consists of a quartz transducer bonded to the (111) face of a crystal of germanium, known to be a good material for acousto-optical modulation at the 10 μm wavelength range.[8] Ultrasonic waves of frequency ω_s are set up in the crystal by means of the transducer, which then scatters part of the laser beam into a single sideband shifted from the laser frequency by ω_s. (Fig. 1) The sign of the shift is determined by choosing the appropriate angle between the acoustic wave and the light beam. A typical value for the conversion efficienty is 1%, obtained at an ultrasonic frequency of 100 MHz. Based on the acccustical properties of germanium, frequency shifts of up to ± 500 MHz are possible[8], as compared with the ± 40 MHz tunability of the CO_2 laser itself.

The CW CO_2 laser and the absorption cell used in these experiments were the same as described earlier. The absorbed signal was measured using a Cu:Ge detector. In order to enhance the signal-to-noise ratio the detector cutput was fed into a lock-in amplifier and then to a waveform eductor. It was convenient to tune the source by first choosing a particular sideband frequency and then tuning the laser frequency by varying the mirror spacing

with a PZT crystal. Thus continuous tunability was achieved even though the acoustic modulation frequency was varied in steps (20 MHz in our case). In this way the center of the D_2O line was found to lie 318 $\pm$ 6 MHz above the center of the 9.6 μm R(22) CO_2 laser transition, whose frequency is accurately known.[3] The center frequency of the $000,5_{33}$ - $010,4_{22}$ D_2O transition was thus determined to be 1079.8628 $\pm$ .0002 cm^{-1}. This accurate value may be useful as a frequency callibration standard.

Oscilloscope traces of the absorption signal observed for sideband frequencies of 310 and 330 MHz are shown in Fig. 2. Note that the absorption peak shifts in the two cases, as expected. From traces of this type the Doppler broadened absorption coefficient at the D_2O center frequency was found to be 0.26 $\pm$ 0.04 cm^{-1} $torr^{-1}$. From this value, the measured detuning, and the absorption coefficient obtained at the laser frequency, the linewidth contribution (HWHM) due to pressure broadening was found to be 13 $\pm$ 3 MHz / torr. This is comparable to the value of 14 MHz / torr for H_2O measured at 5.3 μm[9]. The absorption coefficient measured at the D_2O center frequency corresponds to a dipole moment matrix element of 0.036 Debve for the $000,5_{33}$ - $010,4_{22}$ transition.[10]

Acousto-optic modulation is a general technique which may be used to extend the tuning range of molecular lasers throughout the infrared. It should also be noted that optically pumped molecular systems such as D_2O are suitable for studies of Dicke superradiance.[11]

It is a pleasure to acknowledge the assistance of Ramesh Sharma, J.K.G. Watson, L.W. Ryan, Jr., and Joel Goodrich in the course of this work.

REFERENCES

1. F. Keilmann, R.L. Sheffield, J.R.R.Leite, M.S. Feld, and A. Javan, International Conference on Submillimeter Waves and Their Applications, paper IX-3, Atlanta, June, 1974.
2. In assigning the transitions we have used the spectroscopic data from J.G. Williamson, Ph.D. Thesis, Ohio State University, 1969 (unpublished).
3. K.M. Baird, H.D. Riccius, and K.J. Siemson, Opt. Comm. 6, 91 (1972).
4. H.R. Fetterman, H.R. Schlossberg, and J. Waldman, Opt. Comm. 6, 156 (1972).
5. We are indebted to F. Brown and S. Kronheim of the National Magnet Laboratory for making available their high power optical pumping experiment: F. Brown, S. Kronheim, and E. Silver, International Conference on Submillimeter Waves and their Application, paper VII-1, Atlanta, June, 1974.
6. N. Skribanowitz, M. Kelly, and M.S. Feld, Phy. Rev. A6, 2302 (1972).
7. This modulation technique has recently been used to study narrow laser induced resonances in NH_3: A.T. Mattick, A. Sanchez, N.A. Kurnit, and A. Javan, Appl. Phys. Lett. 23, 675 (1973).
8. R.L. Abrams, D.A. Pinnow, J. Appl. Phys. 41, 2765 (1970).
9. R.S. Eng, A.R. Calawa, R.C. Harman, P.L. Kelley, and A. Javan, Appl. Phys. Lett., 21, 303 (1972).

10. To extract the transition dipole moment from this matrix element it is necessary to take into account effects of centrifugal distortion, which can be large. See for example: Y. Ben Aryeh, J.O.S.A., 60, 1469 (1970). The authors are grateful to S.A. Clough of Air Force Cambridge Research Laboratories for his comments on this point.

11. N. Skribanowitz, I.P. Herman, J.C. MacGillivray, and M.S. Feld, Phys. Rev. Lett., 30, 309 (1973).

Figure Captions

Figure 1: Experimental setup for the acousto-optic modulation and detection of the CW CO_2 laser radiation.

Figure 2: Transmitted CO_2 laser intensity vs. CO_2 laser tuning for two values of accoustic frequency offset. The frequency scale is 20 MHz/division. The broken line indicates the center frequency of the D_2O resonance. The dotted line indicates the center frequency of the CO_2 laser sideband. (a) and (b): D_2O pressure 40 mtorr, transmittance $\sim$20%. (c) and (d): D_2O pressure 80 mtorr, transmittance $\sim$ 4%. Note that in the traces in the first column (accoustic offset: + 310 MHz) the absorption maximum occurs to the right, while in the second column (offset: + 330 MHz) it is shifted to the left. In this way the D_2O molecular center frequency is found to lie 318 MHz above the center of the 9.6 μm R(22) CO_2 laser line.

TABLE I

CO_2 Laser Line	Wavelength (microns)	Absorbing Molecule	Pressure (torr)	Absorption Coefficient α (in units of 10^{-4}/ cm)
R(22)	9.26	D_2O	1	10
R(12)	9.32	D_2O	1	0.5
P(32)	9.66	D_2O	1	1
R(18)	10.26	D_2S	100	25
R(12)	10.30	HDS	6 (a)	5

Table I

Experimentally determined absorption coefficients, α , for water vapor and hydrogen sulfide. Values of α are measured at the center frequencies of the CO_2 laser lines.

(a) Six torr is the partial pressure of HDS, as analyzed by a mass spectrometer, in a 100 torr mixture of H_2S, H_2O, HDS, HDO, D_2O resulting from a reaction of D_2O, H_2SO_4 and FeS.

TABLE II

CO_2 Laser Line		Absorbing Vibrational Transition[b]			Branching Rotational Transition[b] (010 vibrational state)		Observed Submillimeter Emission	
Wavenumber[a] (cm^{-1})	Assignment	Wavenumber (cm^{-1})	Assignment lower level 000	Assignment upper level 010	Wavenumber (cm^{-1})	Assignment	Wavenumber (cm^{-1})	Relative Polarization
1035.47	P(32)	1035.46	7_{34}	6_{25}	85.86	$6_{25} - 5_{14}$	84	∥
1053.92	P(12)	1053.96	--		--	--	--	--
1071.88	R(10)	1071.97	6_{34}	5_{23}	27.66	$5_{23} - 5_{14}$	--	--
1073.28	R(12)	1073.28	--		--	--	70	⊥
1079.85	R(22)	1079.86[c]	5_{33}	4_{22}	26.00	$4_{22} - 4_{13}$	26	⊥
1084.64	R(30)	1084.64	10_{29}	$10_{1\,10}$	101.10	$10_{1\,10} - 9_{09}$	--	∥
1085.77	R(32)	1085.75	9_{09}	8_{18}	82.31	$8_{18} - 7_{07}$	86	∥
1086.87	R(34)	1086.97	4_{31}	3_{22}	39.45	$3_{22} - 3_{13}$	38	∥
1090.03	R(40)	1090.00	--		--	--	--	--

Table II

Identification of absorbing transitions and optically pumped branching transitions in D_2O.

(a) K.M. Baird, H.D. Riccius and K.J. Siemsen, Opt. Comm. 6, 91 (1972).

(b) J.G. Williamson, Ph.D Thesis, Ohio State University, 1969 (unpublished).

(c) From this work we find the center frequency of the $(000,5_{33}) - (010,4_{22})$ transition to be $1079.8628 \pm .0002$ cm^{-1}.

Figure 1

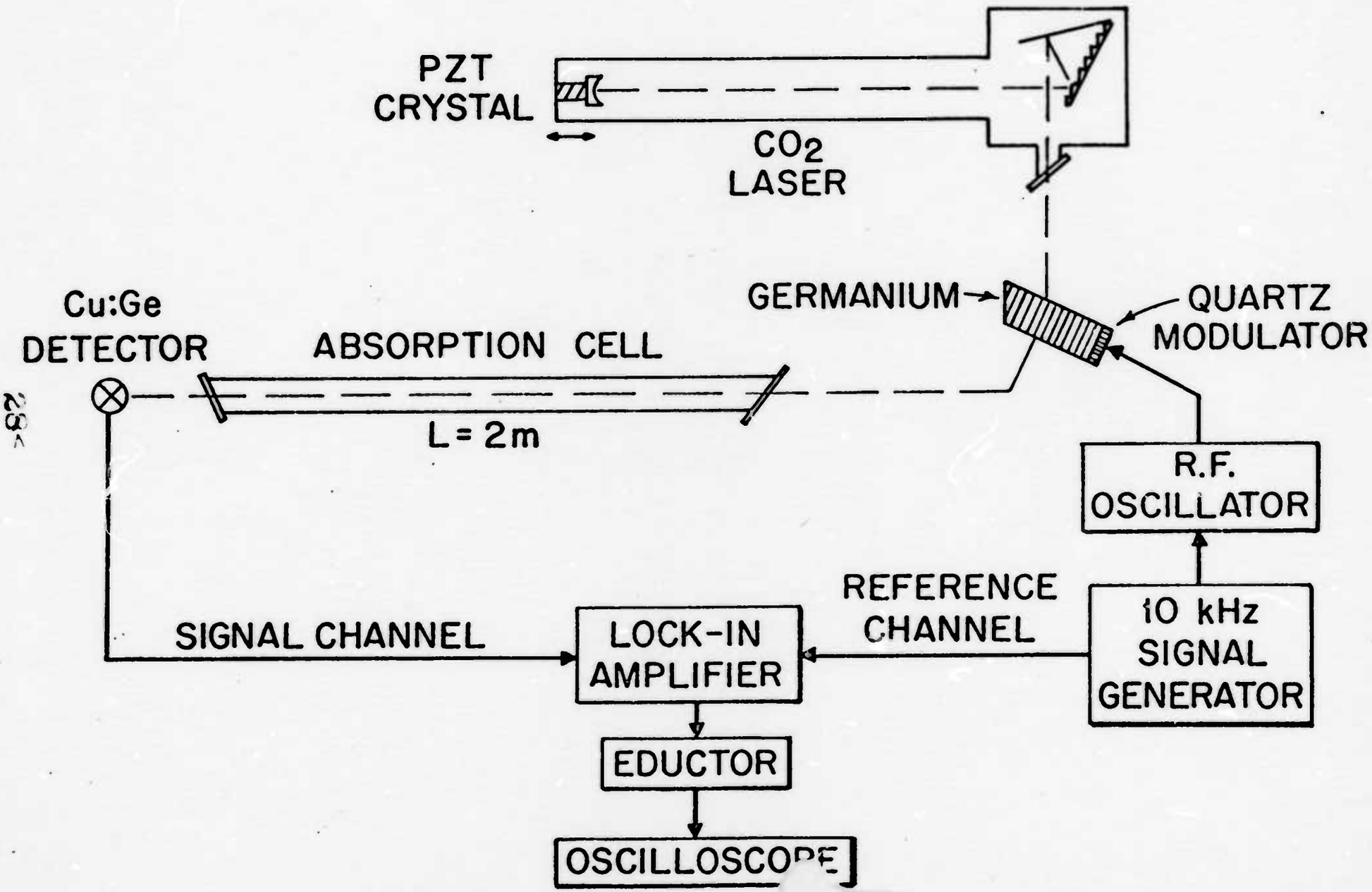
PZT
CRYSTAL
CO_2
LASER
GERMANIUM
QUARTZ
MODULATOR
Cu:Ge
DETECTOR
ABSORPTION CELL
L = 2m
R.F.
OSCILLATOR
REFERENCE
CHANNEL
SIGNAL CHANNEL
LOCK-IN
AMPLIFIER
10 kHz
SIGNAL
GENERATOR
EDUCTOR
OSCILLOSCOPE

Figure 2

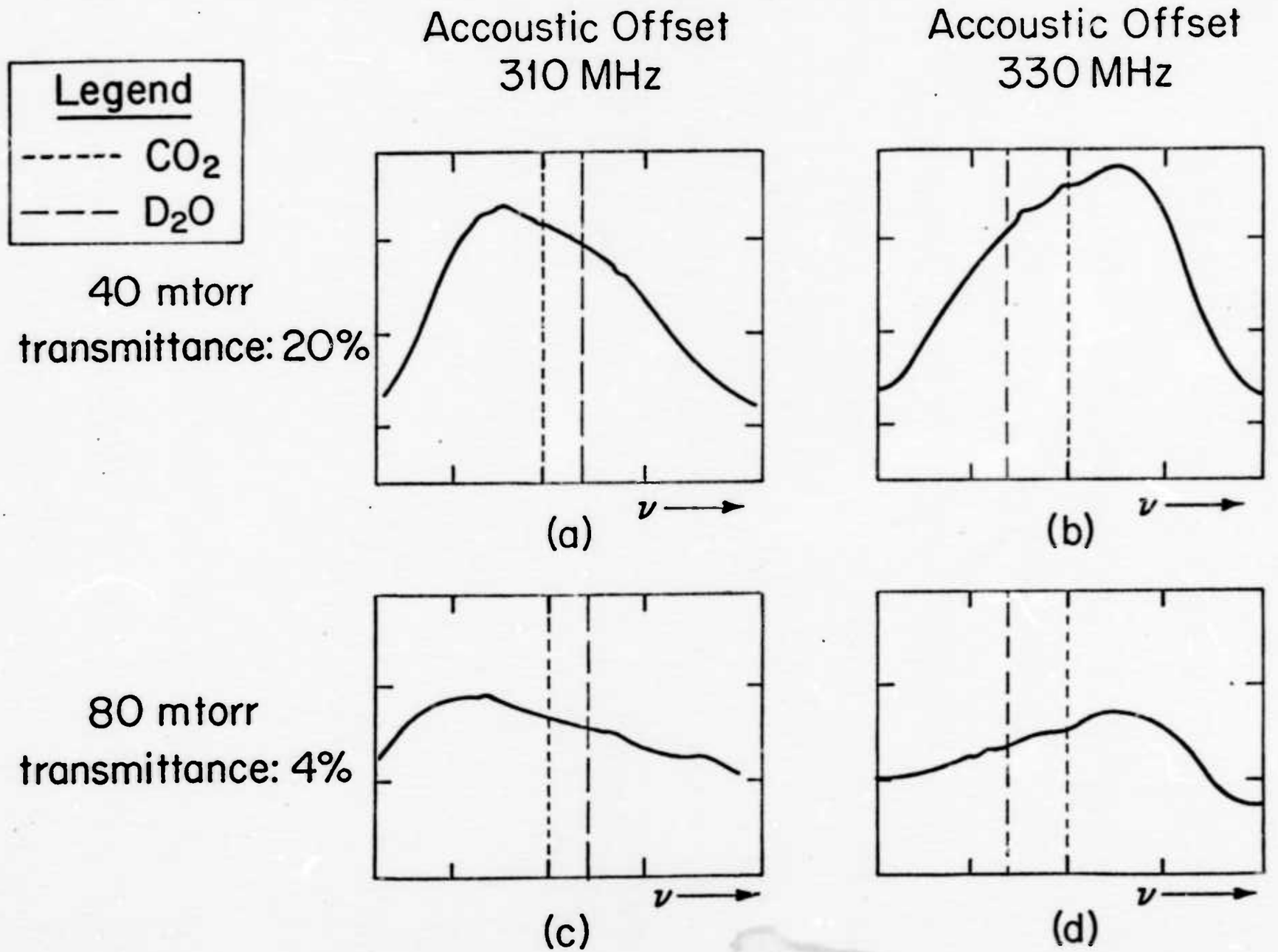
Legend
CO2
D2O
Accoustic Offset
310 MHz
Accoustic Offset
330 MHz
40 mtorr
transmittance: 20%
80 mtorr
transmittance: 4%
ν
(a)
(b)
(c)
(d)

APPENDIX 2

Collision Induced Absorption In He-Ar Mixture

Ramesh D. Sharma

and

Robert R. Hart

ABSTRACT

The absorption coefficient for the collision induced absorption (CIA) in a He - Ar mixture is calculated for frequencies between 67 cm^{-1} - 733 cm^{-1} in the 200 - 400° K temperature range. Starting with a Lennard - Jones (6 - 12) interatomic potential derived from atomic beam work, the absorption coefficient is computed for five different dipole moment functions. The calculation is quantum mechanical, dynamically exact, and uses no adjustable parameters. The results are compared with the room temperature experimental results as well as with previous theoretical work.

Introduction

The collision induced absorption (CIA) in He - Ar mixtures has been the subject of a number of experimental studies. The phenomenon was first discovered by Kiss and Welsh[1] who showed that (1) the absorption in the 350-700 cm^{-1} range was continuous and without any structure, and (2) the absorption coefficient scaled as the product of the two gas densities. Bosomworth and Gush[2] have confirmed the He - Ar results of Kiss and Welsh and have extended the observations down to about 40 cm^{-1}. Reliable experimental results from the CIA for He - Ar mixture are thus available in the 40-700 cm^{-1} region.

Theoretical work on this problem is based upon two approaches. In the statistical approach, an expression for the auto-correlation function of the dipole moment is obtained in terms of a few parameters, which are determined from the experimental data. If these parameters are similar from one pair of inert gases to another, one would say that the underlying model is reasonable. The hope in this type of calculation is that after some experience the details of the absorption process can be predicted for varied species and circumstances. The other approach is dynamical, calculating the CIA from the detailed dynamics of the collision process. This method itself is applied in two ways, one with simplifications in the collision dynamics, the other from a more a priori standpoint. The first of these is used by Levine and Birnbaum, and by Levine,[4] who approximate the interatomic trajectory during the collision by a straight path. The straight path permits the atoms to come much closer than a realistic potential would. To compensate for this, these authors pick a dipole moment

function $\mu(r) = Are^{-Br^2}$, where r is the interatomic distance and A and B are adjustable parameters. This form of dipole moment function has no physical justification, but the factor of r decreases the importance of those collisions in which the atoms have a small impact parameter. The resulting dipole moment autocorrelation function is in surprisingly good agreement with that obtained by Sears.[3]

Also simplifying the dynamics is the work of Tanimoto.[5] He uses a more realistic exponential repulsive potential, i.e., $V(r) = Ae^{-\alpha r}$, and simplifies the dynamics by using the modified wave number approximation. This approximation replaces

$$k^2 - \frac{\ell(\ell+1)}{r^2}$$

in the wave equation for radial motion by $k^2 - \frac{\ell(\ell+1)}{r_{o\ell}^2} = k_\ell^2$,

where $r_{o\ell}$ is the classical turning point for the ℓth partial wave. The radial equation reduces to an s-wave equation with energy of relative motion $\frac{h^2k_\ell^2}{2M}$, and can be solved anaytically for exponential repulsive potentials, $V(r) = Ae^{-\alpha r}$. Further, the integrals over the dipole moment function can be obtained and evaluated in closed form if $\mu = A_1e^{-\alpha_1 r}$, where $\alpha_1 = \alpha$ or $\alpha_1 = \alpha/2$, and α is the range parameter in the interatomic potential. Tanimoto[5] obtains good agreement with the data of Kiss and Welsh in the 350 -- 700 cm^{-1} range. However, his predictions for lower frequencies are not borne out by the experimental work of Bosomworth and Gush.

Also using the dynamical approach with simplified dynamics are Okada, Kajikawa, and Yamamoto.[6] These authors approximate the interatomic potential by a hard sphere, i.e., $V(r) = 0$ for $r > d$, and $V(r) = \infty$ for $r \leq d$. Assuming a dipole moment function $\mu(r) = A_2 e^{-\alpha_2 r}$, and using classical mechanics to describe the atomic motion, they calculate the CIA for Ne -Ar and He - Ar mixtures. The two adjustable parameters in the dipole moment function are obtained from the low frequency region of the experimental work of Bosomworth and Gush. The hope and expectation for the adjustable parameters are the same as in statistical calculations.

In the second, more a priori, method within the dynamical approach, the starting point is the interatomic potential and dipole moment function, obtained from independent sources. Using classical or quantum equations of motion, the expectation value of the dipole moment, and hence the absorption coefficient, is then computed. The work of McQuarrie and Bernstein[7] on CIA in He - Ar is in this spirit. These authors used a Lennard-Jones 6-12 potential to describe the He-Ar interaction. The parameters used, $\varepsilon = 3.50 \times 10^{-15}$ ergs and $\sigma = 3.07\text{Å}$, are derived from molecular beam measurements of Düren, Feltgen, Gaide, Helbing and Pauly.[8] The dipole moment function is taken from ab initio calculations of Matcha and Nesbet.[9] With these input parameters, and using the classical equations of motion to calculate the trajectories, the dipole moment function induced during the collision can be calculated and its Fourier transform obtained. The absolute square of the Fourier component at frequency ω gives, aside from constant factors, the absorption coefficient at this frequency. These authors have computed the absorption

coefficient only for frequencies less than $\sim 240\ cm^{-1}$, due to slow convergence of some of the integrals. The results of this study, which computes the absorption coefficient for free-free transitions, are smaller than experiment by a factor of about three, but can be brought into agreement with experiment if the value of the range parameter ρ in the dipole moment correlation function $\mu(r) = \mu_0 e^{-r/\rho}$, is increased by about 8% from the value calculated by Matcha and Nesbet.[9] The predictions of these authors on the temperature dependence of the absorption coefficient have not been tested experimentally. The drawback of this classical calculation is that it does not conserve energy. The energy of the system does not change after absorption of the photon.

In this paper we present a calculation of the He - Ar absorption coefficient in the McQuarrie-Bernstein spirit, but using quantum instead of classical mechanics, and conserving energy. The quantum-mechanical wave functions are used to compute the expectation value of the dipole moment function between initial and final states. This calculation, which treats the collision dynamics exactly, should give results whose accuracy is limited only by that of the two inputs (interatomic potential and dipole moment function), and by the numerical accuracy of the calculation. We thus believe that this approach has the advantage, that given reliable CIA experimental data and one of the two input parameters, this calculation can be used to test the proposed values of the other input parameter. For example, there have been proposed two very different dipole moment functions due to overlapping of atomic charges for the He-Ar pair.[9,10] Although both dipole moment calculations involve serious approximation, we believe that reliable experimental data on CIA

in He - Ar mixtures might provide some evidence concerning the dependability of these approximations. There is in addition a detailed calculation of the long-range r^{-7} dipole moment function induced by dispersion forces alone.[11] This function is 6.6 times smaller and opposite in sign to that obtained by Levine[12] for the same quantity, using a simple Drude model.

Another advantage of the present approach is that it can provide an independent check of the experimental data. For example, Kiss and Welsh[1] measured the absorption coefficient for the 1:1 He - Ne mixture to be 2.6×10^{-7} and 0.7×10^{-7} cm^{-1} $amagat^{-2}$ at 400 cm^{-1} and 600 cm^{-1}, respectively. Although the failure of Bosomworth and Gush to obtain measurable absorption around 200 cm^{-1} cast some doubt on the He - Ne results of Kiss and Welsh, it was a calculation in this same spirit[12] which pointed out that the Kiss-Welsh results may be in error by about two orders of magnitude. Although the calculation is probably more laborious and certainly more expensive than the ones described earlier, we believe the reliability of the results, and the opportunity it affords to test more approximate models, justifies the additional expense.

II. Absorption Coefficient for Free-Free Transitions

The transition probability P, i.e., number of transitions per second between an initial state i and final state f is given, according to Fermi's Golden Rule, by

$$P = \frac{2\pi}{\hbar} \left| \langle f \left| V \right| i \rangle \right|^2 \delta(E), \qquad (1)$$

where V is the external perturbation and the Dirac delta function insures conservation of energy. If the perturbation connects multiple

initial and final states, expression (1) is modified to

$$P = \frac{2\pi}{\hbar} \sum_i \sum_f p_i \left| \langle f|v|i\rangle \right|^2 \delta(E) \tag{2}$$

where p_i is the probability the system is in the state i and $\Sigma_i\, p_i = 1$. For a perturbation due to an electromagnetic field of frequency ω

$$V = -\underline{\mu} \cdot \underline{E} = -\frac{E_o}{2} \underline{\mu} \cdot \hat{\underline{\epsilon}} \, (e^{i\omega t} + e^{-i\omega t}), \tag{3}$$

where μ is the dipole moment of the system and $\hat{\underline{\epsilon}}$ is a unit vector in the direction of the electric field of the incident photon. Substituting in (2), we get

$$P = \frac{\pi}{\hbar} E_0^2 \sum_i \sum_f p_i \left| \langle f|\underline{\mu}.\hat{\underline{\epsilon}}|i\rangle \right|^2 (\delta(E_f - E_i - h\omega) + \delta(E_f - E_i + h\omega)) \tag{4}$$

The first delta function in Eq. (4) corresponds to absorption while the second one corresponds to stimulated emission. The second term is also sometimes called the non-resonant term.

To see this quantitatively, we write the expression for the power absorbed per second, $\dot{I}$, by the system

$$\dot{I} = -h\omega P = \frac{\pi}{2} E_0^2 \left(\sum_{i,f} (E_f - E_i) p_i \left| \langle f|\underline{\mu}.\hat{\underline{\epsilon}}|i\rangle \right|^2 \delta(E_f - E_i - h\omega) + \sum_{i,f} (E_i - E_f) p_i \right.$$
$$\left. \left| \langle f|\hat{\underline{\mu}} \cdot \hat{\underline{\epsilon}}|i\rangle \right|^2 \delta(E_f - E_i + h\omega) \right). \tag{5}$$

Interchanging the dummy indices i and f in the second sum on the right-hand side of Eq. (5) and recalling that $|\langle f|\ \underline{\mu}\ .\ \underline{\hat{\varepsilon}}|i\rangle|^2 = |\langle i|\underline{\mu}\ .\underline{\hat{\varepsilon}}|f\rangle|^2$, and that $x\delta(a+x) = -x\delta(a-x)$, we get

$$\dot{I} = -\frac{\pi}{2}\ \omega E_0^2 \sum_{i,f} (p_i - p_f) |\langle f|\underline{\mu}\ .\ \underline{\hat{\varepsilon}}|\ i\rangle\ |^2\ \delta(E_f - E_i - h\omega) \qquad (6)$$

In this form it is clearly seen that the term involving p_f is the stimulated emission term. The absorption coefficient $\alpha(\omega)$ at frequency ω in units of cm^{-1} amagat^{-2}, is given by

$$\alpha(\omega) = -n_L^2\ \dot{I} \times \frac{8\pi}{E_0^2 c}$$

$$= \frac{4\pi^2}{c}\ \omega n_L^2 \sum_{i,f} (p_i - p_f) |\langle f|\underline{\mu}\ .\ \underline{\hat{\varepsilon}}|i\rangle|^2\ \delta(E_f - E_i - h\omega) \qquad (7)$$

where $n_L = 2.687 \times 10^{19}$ is the number of atoms/cc at S.T.P. (Loschmidt's number).

For the wavefunctions of the relative translational motion, we take

$$|\ i\ \rangle = \frac{4\pi}{kr} \sum_{\ell} i^{\ell} e^{i\delta_\ell}\ R_\ell(kr) \sum_m Y^*_{\ell m}(\hat{\underline{k}})\, Y_{\ell m}(\hat{\underline{r}}) \qquad (8)$$

where r and $\hat{r}$ denote the magnitude and orientation of the distance between two nuclei; k and $\hat{k}$ denote similar quantities for the wave vector of relative motion, $Y_{\ell m}$ are spherical harmonics and $R_\ell(kr)$ is the solution of the differential equation.

$$\frac{d^2}{dr^2} R_\ell(kr) + \left(k^2 - \frac{\ell(\ell+1)}{r} - \frac{2M}{\hbar^2} V(r) \right) R_\ell(kr) = 0 \tag{9}$$

with boundary conditions

$$\lim_{r \to 0} R_\ell(kr) = 0 \tag{9a}$$

and

$$\lim_{r \to \infty} R_\ell(kr) = \sin\left(kr - \frac{\ell\pi}{2} + \delta_\ell\right), \tag{9b}$$

where δ_ℓ is the phase shift of the ℓth partial wave potential $V(r)$ at energy $\frac{\hbar^2 k^2}{2M}$.

In writing Eqs. (7) and (8) we have factored out the motion of the center of mass of the two atoms. We thus ignore the Doppler effect throughout the present work.

In the absence of a potential the wave function i becomes a plane wave, i.e., $\lim_{V \to 0} |i\rangle = e^{i\underline{k}\cdot\underline{r}}$. Because the potential V(r) does not create or destroy particles, it conserves normalization, permitting us to calculate the incident and outgoing fluxes using plane waves.

p_i, the probability of two atoms colliding with relative momentum between $\hbar\underline{k}_i$ and $\hbar(\underline{k}_i + d\underline{k}_i)$ is given by

$$p_i = \frac{(2\pi)^{-3} k_i^3 \, dk_i \, d\Omega(\hat{k}_i) \exp\left[-\frac{\hbar^2 k_i^2}{2M}\beta\right]}{\frac{4\pi}{(2\pi)^{-3}} \int_0^\infty k^3 dk \exp\left[-\frac{\hbar^2 k^2}{2M}\beta\right]}$$

$$= \frac{1}{2\pi}\left(\frac{\beta\hbar^2}{2M}\right)^2 k_i^3 \exp\left[-\beta\frac{\hbar^2 k_i^2}{2M}\right] dk_i \, d\Omega(\hat{k}_i) \qquad (10)$$

where $\beta = \frac{1}{k_B T}$, k_B is the Boltzmann constant, and T is the temperature in degrees Kelvin. The factor $(2\pi)^{-3}$ comes from the fact that for unit volume, the number of states in the interval $\underline{k}$ and $\underline{k} + d\underline{k}$ is $\frac{k^2 dk d\Omega}{(2\pi)^3}$. The sum over the final states is written as

$$(2\pi)^{-3} \int_0^\infty k_f^2 \, dk_f \int d\Omega_f \qquad (11)$$

Equations (10) and (11) differ by a factor k because the probability that two atoms collide is taken to be $kf(\underline{k})$, where $f(\underline{k})$ is the distribution function. From Eqs. (7) - (11) we get

$$\alpha(\omega) = \frac{16\pi^2}{3c} \omega n_L^2 \beta^2 \hbar (2M)^{-\frac{1}{2}} \int_0^\infty dE (E+\hbar\omega)^{-\frac{1}{2}} e^{-\beta E}\left[1-(1+\frac{\hbar\omega}{E})^{\frac{1}{2}} e^{\beta\hbar\omega}\right] \times I(k_i, k_f), \qquad (12)$$

where

$$I(k_i, k_f) = \sum_\ell \left(\ell I_{\ell,\ell-1} + (\ell+1) I_{\ell,\ell+1}\right) \qquad (13)$$

is the sum over partial waves, and

$$I_{\ell,\ell_1} = \left(\int_0^\infty R_\ell(k_i r) \, R_{\ell_1}(k_f r) \, \mu(r) dr\right)^2, \qquad (14)$$

where $\mu(r)$ is the dipole moment function, and k_f is determined by the energy conservation relation

$$k_f = \left(k_i^2 + \frac{2M\omega}{\hbar}\right)^{1/2} .$$

III. Bound to Free Transitions:

In this type of transition the two atoms form a molecule in the initial state. This molecule may be a true bound state with negative energy, or it may be a positive energy state trapped in the centrifugal barrier (resonant state). In either case, an absorption process corresponds to photodissociation of the molecule. Because the He -- Ar potential has a well-depth of only about 17.5 cm^{-1}, He - Ar has only one bound vibrational state, which supports five rotational states. Their energies, calculated using L-J (6-12) potential,

$$V(r) = \varepsilon\left[\left(\frac{r_m}{r}\right)^{12} - 2\left(\frac{r_m}{r}\right)\right]^6 ,$$

with $\varepsilon = 0.350 \times 10^{-14}$ ergs and $r_m = 3.45$ Å, are -5.756, -5.178, -4.039, -2.377, and -0.272 cm^{-1}.

The wavefunction for the bound state $|b_{\ell m}\rangle$ can be written in the form

$$|b_{\ell m}\rangle = \frac{1}{r} R_\ell(kr) Y_{\ell m}(\Omega r) , \qquad (15)$$

where the vibrational wavefunction $R_\ell(kr)$ is solution of the wave equation

$$\frac{d^2}{dr^2} R_\ell(kr) - \left[k^2 + \frac{\ell(\ell+1)}{r^2} + \frac{2M}{\hbar^2} V(r)\right] R_\ell(kr) = 0 \qquad (16)$$

with boundary conditions

$$\lim_{r \to 0} R_\ell(kr) = 0 \tag{16a}$$

and

$$\lim_{r \to \infty} R_\ell(kr) = 0 \ . \tag{16b}$$

The binding energy E of this state is $E_b = -\frac{\hbar^2 k^2}{2M}$. The $b_\ell(kr)$ functions are assumed ortho-normal, i.e., $\langle b_\ell(kr) | b_{\ell'}, (k'r) \rangle = \delta_{\ell\ell'}\delta_{kk'}$.

The probability p_i for the two atoms to be initially in the bound state is

$$p_i = \frac{e^{-\beta E_i}}{\left(\frac{M}{2\pi\beta\hbar^2}\right)^{3/2} + \sum_i (2\ell_i + 1) e^{-\beta E_i}} \tag{17}$$

The sum over the final states is given by Eq. 11. For the reverse process, i.e., stimulated free-bound emission, $p_i^{(r)}$ is given by Eq. 10, whereas the sum over the final states for the reverse process is just the sum over the bound states, i. e.,

$$\sum p_f^{(r)} = \sum_i \ . \tag{18}$$

Substituting Eqs. (10), (11), (17) and (18) in Eq. (7), and substituting initial and final state wavefunctions from Eqs. (15) and (8), respectively, we get, after some algebra.

$$\alpha(\omega) = \frac{2\pi}{c}\ \omega n_L^2 \left(\frac{\hbar^2}{2M}\right)^2 \sum_i \left[Q_i \left(\frac{8M}{\pi\beta\hbar^2}\right)^{1/2} e^{-\beta E_i} \int_0^\infty k_f^2 dk_f \int d\Omega_f \right.$$

$$\left. - \int_0^\infty k_f^3 dk_f\ e^{-\beta E_f} \int d\Omega_f \right] \left| \langle f \mid \underline{\mu}\cdot\underline{\varepsilon} \mid b_{\ell m}(k) \rangle \right|^2 \delta(E_f - E_i - \hbar\omega) \qquad (19)$$

where

$$Q_i \equiv \left[1 + \left(\frac{M}{2\pi\beta\hbar^2}\right)^{-3/2} \sum_i (2\ell_i+1)\ e^{-\beta E_i} \right]^{-1} \qquad (20)$$

$$\alpha'(\omega) = \frac{8\pi^3}{3c}\ \omega n_L^2 \beta^2 \hbar^2 M' \sum_i e^{-\beta E_i} \left[2Q_i (\pi\beta)^{-1/2} (\hbar\omega + E_i)^{-1/2} - e^{-\beta\hbar\omega} \right]$$

$$\times \quad I(k_b, k_f) \qquad (21)$$

where the function $I(k_b, k_f)$ is defined in Eqs. (13) and (14) with the change that $R_\ell(k_b r)$ satisfies differential equation and boundary conditions given by Eq. (16).

IV. Computations

The dipole transition probabilities to be evaluated are of the form

$$\sum_{\ell=0}^{N} \left[\ell I_{\ell,\ell-1} + (\ell+1)\, I_{\ell,\ell+1} \right] . \tag{22}$$

Typical values of N required for convergence of the sum to three figures are 50. The integrals are

$$I_{\ell,\ell'} = \left(\int_0^{\infty} R_{\ell}(k_i r)\, R_{\ell'}(k_f r)\, \mu(r)\, dr \right)^2 , \tag{23}$$

where $\mu(r)$ is the collision-induced dipole moment, and $R_{\ell}(k_i r)$ and $R_{\ell'}(k_f r)$ are the radial wave functions of the initial and final states, of angular momentum quantum numbers ℓ and ℓ'. The five forms of $\mu(r)$ for which we calculated the CIA are defined in Table I.

The integrals are calculated in straightforward fashion, first obtaining the wave functions and then evaluating the integrals by Simpson's rule.

The wave functions are stored on tape for re-use. The wave functions are calculated for each ℓ using the double-precision program DHPCG from the IBM Scientific Subroutine Package. This solves differential equations numerically using a Milne-Hamming predictor-corrector method. This is a stable, fourth-order "stepping" method (i.e., using given initial values, as distinct from boundary conditions), with good error control.

The differential equations to be solved are the standard radial part of the Schrödinger equation (Eq. 9), with the given interatomic potential. The solution must be known at some point to provide initial values. This point is taken far enough inside the classically forbidden region that the wave function is essentially zero, and the equation integrated outward from there. This yields a solution to within normalization, with the normalization factor easily found after the solution has attained the asymptotic limit,

$$R_\ell(kr) \xrightarrow[k \to \infty]{} \sin\left(kr - \frac{\ell\pi}{2} + \delta_\ell\right), \tag{24}$$

where δ_ℓ is the phase shift of the ℓ-th partial wave. For a minimum in the He-Ar interatomic potential at 3.45×10^{-8} cm, typically 750 points of the wave function are stored, out to a distance of 50×10^{-8} cm. Error control, to attain the desired three-figure accuracy in the final sum over integrals, was done experimentally: by adjusting the wave function tolerance which is input to the program DHPCG; by altering the intervals at which the wave functions are stored, for input to the Simpson's rule integration; and by observing how high ℓ must be carried in the final sum. Typical IBM 370-165 CPU times for calculating fifty wave functions for $\ell = 0 \to 50$, for a single initial or final state (i.e., a single energy), are five minutes, with ten minutes thus required for an entire sum over integrals. This approach is simple and

direct, with maximum use of stock "library" programs; but probably at the expense of greater efficiency attainable from programs tailored for these calculations.

The five bound state energies were obtained using essentially the same programs as were used to calculate the wave functions. The simple scheme was merely to iteratively adjust the energies (now negative instead of positive) in the radial part of the Schrödinger equation (Eq. 16), until the wave function yielded by the calculation obeyed as well as possible the boundary condition given by Eq. (16b).

IV Results and Discussion

It was pointed out earlier that the most tightly bound state of He-Ar has a binding energy of about 6 cm^{-1}. According to Eq. (17), the probability for the occurrence of this state is $\left(\frac{M}{2\pi\beta\hbar^2}\right)^{-3/2}$. This probability is about 10^{-6} time the probability (Eq. 10) that He and Ar collide with thermal energy. Since the integrals over transition moments have similar magnitude, the result is that the contribution of bound-free transitions to CIA in He-Ar is much smaller than the contribution of the free-free transitions. In fact, the uncertainty introduced in the free-free CIA due to computational procedures far exceeds the contribution due to bound-free transitions. We will therefore ignore the bound-free contribution.

Ideally, the dipole moment function for He-Ar should be calculated in a manner which takes electron correlation into account, such as a Hartree-Fock calculation including configuration interaction. Such a calculation is presently unavailable. There are three approximate calculations of dipole moment function available in the literature.

On the one hand is the molecular Hartree-Fock calculation of Matcha and Nesbet (M-N)[9], which is probably a better picture of the real situation at small internuclear distances. On the other hand is the calculation of Lacey and Byers Brown[10] (L-BB), which approximates the overlap contribution to the dipole moment by electron exchange between undistorted Hartree-Fock atoms. Because these calculations involve different assumptions, it is not unreasonable to assume that each one may be a better representation of the physical situation in a restricted interval.

Neither of these calculations includes the contribution of the dispersion forces to the dipole moment function. The leading dispersion term in the dipole moment function has been computed by Whisnant and Byers Brown[11] (W-BB). In this work we will calculate the CIA due to these three dipole-moments functions, as well as the two dipole-moment functions obtained by adding the W-BB dispersion contribution to the M-N and L-BB overlap contributions.

This simple addition of overlap and dispersion parts has scant theoretical justification. However, this customary procedure is the best currently available. It yields the correct dipole moment function at large internuclear distances where the dispersion term dominates, and, at the smallest internuclear distances realized in the collisions presently under consideration, where the overlap term dominates, reduces to the desired M-N or L-BB overlap form.

Several potential functions for He-Ar have been proposed. Matcha and Nesbet[9], from their molecular Hartree - Fock calculation discussed earlier, proposed an exponential repulsive potential for the inert gas atoms. Colgate et al.[14], and Kenney and Leonas[15] have investigated the He-Ar potential for energies in the 1 eV range, i.e., about 8000 cm^{-1}. However, since we will deal with relative energies in the 200-1200 cm^{-1} range, these results are not useful to us. Walker and Westenberg[16] have interpreted their diffusion work (300-1000° K) assuming only a repulsive part for the He-Ar potential.

In the present study we will use the potential arrived at from the molecular beam work of Düren et al.[8] Not only is this investigation in the energy interval of direct interest to us (200-3,000 m/s relative velocity).

but also the results were interpreted using both an attractive and a repulsive part, which is more realistic than a solely repulsive potential. In addition, this potential was also used in the earlier He-Ar CIA work of McQuarrie and Bernstein[7], and thus facilitates comparison with their results.

Finally, in our earlier study on CIA in He-Ne, we directly tested the effect of the potential adopted. The He-Ne potential of Düren et al. was mainly used, but a limited amount of this work was duplicated using the M-N He-Ne potential, with essentially the same results. We believe that in the range of internuclear distances of interest, that this is probably again the case.

Table I gives the results of our calculations at 300° K using the five different dipole moment functions mentioned, and compares them with the experimental work of Kiss and Welsh, and with that of Bosomworth and Gush. We also show the theoretical results of McQuarrie and Bernstein (McQ-B). This calculation uses the same interatomic potential and dipole moment function as our "M-N overlap only" column, and differs from the latter only in using classical instead of quantum mechanics. It is gratifying to note that our results agree with those of McQ-B where one might expect the latter to be most valid, namely at 67 cm^{-1}. The McQ-B calculation does not conserve energy, i.e., the absorbed photon does not affect the translational motion of the atoms—an approximation which should be least serious at small photon energies, and most serious at large, where, indeed, our energy-conserving results differ from McQ-B. In particular, our calculations show that most of the contribution to the absorption coefficient at frequencies below 240 cm^{-1} (where McQ-B obtained their results), comes from atoms colliding with a

relative energy of 300-500 cm^{-1}. While it may be reasonable to take translational kinetic energy as conserved if a 67 cm^{-1} photon is absorbed, this seems less plausible for a 240 cm^{-1} photon.

In the early discussion[12] of the validity of the M-N induced dipole moment function, there figured largely the latter's neglect of the r^{-7} dispersion term. It is interesting that for He-Ar this term is relatively unimportant. Its inclusion or neglect affects the calculated results substantially less than the choice of overlap part: whether L-BB overlap or M-N overlap. Levine,[12] using a simple Drude model, early obtained the result, that the r^{-7} dispersion term in the induced dipole moment by itself accounts for 60-90% of the experimental He-Ar zeroth moment for absorption. By contrast, our corresponding results for the absorption coefficient are nearer 1%. These results given in the"W-BB dispersion only" column of Table I were obtained using the induced dipole moment resulting from the much more sophisticated calculation of BB-W.

Table I shows that for low absorption frequencies, including the bulk of the room-temperature absorption, the L-BB + W-BB induced dipole moment function gives results closer to experiment, than does the M-N + W-BB function; while for high frequencies this situation is reversed. Our experience is that the transition moment integral is largely determined by the magnitude of the induced dipole moment at the classical turning point--presumably because the radial wavefunctions are least rapidly oscillating there. Table I thus implies that the M - N induced dipole moment function is more accurate at internuclear distances equal to the classical turning points associated with high frequencies. These imply high translational energies, and thus generally smaller classical turning points. This is in accord with the expectation that the M-N calculation is most accurate at small distances, and that the L-BB calculation, based on electron exchange between undistorted Hartree-Fock atoms, is more accurate at larger distances. We estimate the distance at which one dipole moment function becomes more accurate than the other, as about 2.4-2.5 Å: The two functions yield about equally accurate results for the 400 cm^{-1} transitions, and the main contributions to this transition come from wave functions corresponding to classical turning points in this range.

In tables II-VI, we give the temperature dependence of absorption coefficient as a function of frequency for the five dipole moment functions, for future comparison with experiment, as well as with more approximate models.

References

1. Z. J. Kiss and H. L. Welsh, Phys. Rev. Letters 2, 166 (1959).
2. D. R. Bosomworth and H. P Gush, Can. J. Phys. 43, 751 (1965).
3. V. F. Sears, Can. J. Phys. 46, 1163 (1968); ibid 46, 1501 (1968).
4. H. B. Levine and G. Birnbaum, Phys. Rev. 154, 86 (1967); H. B. Levine, Phys. Rev. 160, 159 (1967).
5. O. Tanimoto, Prog. Theoretical Physics 33, 585 (1965).
6. K. Okada, T. Kajikawa and T. Yamamoto, Prog. Theoretical Physics 39, 863 (1968).
7. D. A. McQuarrie and R. B. Bernstein, J. Chem. Phys. 49, 1958 (1968).
8. R. Düren, R. Feltgen, W. Gaide, R. Helbing, and H. Pauly, Phys. Letters 18, 232 (1965).
9. R. L. Matcha and R. K. Nesbet, Phys. Rev. 160, 72 (1967).
10. A. J. Lacey and W. Byers Brown, Molecular Phys 27, 1013 (1974).
11. D. M. Whisnant and W. Byers Brown, Molecular Physics 26, 1105 (1973).
12. H. B. Levine, Phys. Rev. Letters, 21, 1512 (1968).
13. R. D. Sharma and R. R. Hart, Chem. Phys. Letters 27, 589 (1974).
14. S. O. Colgate, J. E. Jordan, I. Amdur, and E. A. Mason, J. Chem. Phys. 51, 968 (1969).
15. A. B. Kemnev and V. B. Leonas, Sov. Phys. Doklady 10, 529 (1965).
16. R. E. Walker and A. A. Westenburg, J. Chem. Phys. 31, 519 (1959).

Table I: Values of the collision-induced absorption (10^{-7} cm^{-1} $amagat^{-2}$) for He-Ar mixture at room temperature. The theoretical induced dipole moments are (in atomic units: r in a_o's, $\mu(r)$ in ea_o, a_o = bohr radius, and e = electronic charge; $He^{+}Ar^{-}$ taken as positive):

(1) L-BB. Lacey and Byers-Brown overlap term (read from Fig. 1 of Ref. 10): $\mu_{L\text{-}BB}(r) = 31.6\ e^{-1.530r}$

(2) M-N Matcha and Nesbet overlap term (Fig. 1 of Ref. 9): $\mu_{M\text{-}N}(r) = 13.3\ e^{-1.472r}$

(3) W-BB. Whisnant and Byers Brown dispersion term (Table II of Ref.11) : $\mu_{W\text{-}BB}(r) = -125/r^7$. (Note that this has opposite polarity than the first two.)

Transition Frequency (cm^{-1})	Experimental		Theoretical					
	Kiss and Welsh (Fig. 1a of Ref.1)	Bosomworth and Gush (Fig. 2 of Ref. 5)	Present Calculations L-BB + W-BB	M-N + W-BB	L-BB overlap only	M-N overlap only	W-BB dispersion only	Classical M-N Calculations (Fig. 2 of Ref. 7, ρ^*=0.117)
67	---	3.0	2.6	0.70	3.4	1.1	0.047	1.1
133	---	6.8	6.2	1.6	7.8	2.5	0.086	2.2
200	---	7.5	7.1	1.9	8.8	2.7	0.087	2.2
267	---	5.8	6.4	1.6	7.8	2.4	0.073	1.6(extrapolated)
333	5.2 (extrapolated)	3.7	5.0	1.2	6.2	1.8	0.056	---
400	2.6	2.2	3.7	0.88	4.5	1.3	0.041	---
467	1.2	1.2	2.6	0.61	3.2	0.91	0.029	---
533	0.63	0.63 (extrapolated)	1.8	0.42	2.2	0.63	0.021	---
600	0.35	0.31 (extrapolated)	1.2	0.29	1.5	0.43	0.015	---
667	0.15	---	0.86	0.19	1.1	0.29	0.011	---
733	---	---	0.60	0.13	0.74	0.20	0.0075	---

Table II. Calculated values of the collision-induced absorption (10^{-7} cm^{-1} $amagat^{-2}$) for He-Ar mixture as a function of temperature, calculated from the theoretical induced dipol moment, $\mu(r) = \mu_{L-BB}(r) + \mu_{W-BB}(r)$, as defined in Table I.

Temperature	Transition Frequency (cm^{-1})										
°K	67	133	200	267	333	400	467	533	600	677	733
200	3.1	6.1	5.9	4.6	3.2	2.1	1.4	0.89	0.56	0.37	0.24
250	2.8	6.2	6.6	5.6	4.2	2.9	2.0	1.3	0.88	0.59	0.40
300	2.6	6.2	7.1	6.4	5.0	3.7	2.6	1.8	1.2	0.86	0.60
350	2.4	6.1	7.5	7.1	5.8	4.4	3.2	2.3	1.6	1.2	0.82
400	2.3	6.0	7.7	7.6	6.5	5.1	3.9	2.9	2.1	1.5	1.1

Table III. Calculated values of the collision-induced absorption (10^{-7} cm^{-1} $amagat^{-2}$) for He-Ar mixture as a function of temperature, calculated from the M-N overlap term plus the W-BB dispersion term: $\mu(r) = \mu_{M-N}(r) + \mu_{W-BB}(r)$, as defined in Table I.

Temperature	Transition Frequency (cm^{-1})										
°K	67	133	200	267	333	400	467	533	600	667	733
200	0.83	1.6	1.5	1.2	0.78	0.50	0.32	0.20	0.13	0.082	0.054
250	0.76	1.6	1.7	1.4	1.0	0.69	0.46	0.31	0.20	0.13	0.088
300	0.70	1.6	1.9	1.6	1.2	0.88	0.61	0.42	0.29	0.19	0.13
350	0.65	1.6	1.9	1.8	1.4	1.1	0.77	0.54	0.38	0.26	0.18
400	0.60	1.6	2.0	1.9	1.6	1.2	0.91	0.66	0.47	0.33	0.24

Table IV. Calculated values of the collision-induced absorption (10^{-7} cm^{-1} $amagat^{-2}$) for He-Ar mixture as a function of temperature, calculated from the L-BB overlap induced dipole only: $\mu_{L\text{-}BB}(r)$, as defined in Table I.

Temperature	Transition Frequency (cm^{-1})										
°K	67	133	200	267	333	400	467	533	600	667	733
200	3.9	7.5	7.3	5.6	3.9	2.6	1.7	1.1	0.70	0.45	0.30
250	3.6	7.8	8.2	6.8	5.1	3.5	2.4	1.6	1.1	0.73	0.49
300	3.4	7.8	8.8	7.8	6.2	4.5	3.2	2.2	1.5	1.1	0.74
350	3.1	7.7	9.3	8.7	7.1	5.4	4.0	2.9	2.0	1.4	1.0
400	2.9	7.5	9.5	9.3	7.9	6.3	4.7	3.5	2.6	1.8	1.3

Table V. Calculated values of the collision-induced absorption (10^{-7} cm^{-1} $amagat^{-2}$) for He-Ar mixture as a function of temperature, calculated from the M-N overlap induced dipole only: $\mu_{M-N}(r)$, as defined in Table I.

Temperature	Transition Frequency (cm^{-1})										
°K	67	133	200	267	333	400	467	533	600	667	733
200	1.3	2.4	2.3	1.7	1.2	0.74	0.48	0.31	0.19	0.13	0.082
250	1.2	2.5	2.5	2.1	1.5	1.0	0.69	0.46	0.30	0.20	0.14
300	1.1	2.5	2.7	2.4	1.8	1.3	0.91	0.63	0.43	0.29	0.20
350	1.0	2.4	2.9	2.6	2.1	1.6	1.1	0.81	0.57	0.40	0.28
400	0.95	2.4	2.9	2.8	2.4	1.8	1.4	0.99	0.71	0.51	0.36

Table VI. Calculated values of the collision-induced absorption (10^{-7} cm^{-1} amagat^{-2}) for He-Ar mixture as a function of temperature, calculated from the W-BB dispersion induced dipole only: $\mu_{W\text{-}BB}(r)$, as defined in Table I.

Temperature	Transition Frequency (cm^{-1})										
°K	67	133	200	267	333	400	467	533	600	667	733
200	0.055	0.081	0.070	0.051	0.035	0.023	0.015	0.010	0.0067	0.0045	0.0031
250	0.051	0.085	0.080	0.063	0.046	0.032	0.022	0.015	0.011	0.0072	0.0051
300	0.047	0.086	0.087	0.073	0.056	0.041	0.029	0.021	0.015	0.011	0.075
350	0.043	0.086	0.092	0.081	0.065	0.050	0.037	0.027	0.020	0.014	0.010
400	0.040	0.084	0.096	0.088	0.073	0.058	0.044	0.033	0.025	0.018	0.013

APPENDIX III

WATER VAPOR SPECTROSCOPY AT 5μ USING A TUNABLE SPIN-FLIP RAMAN LASER

M. Guerra, M. Ketabi, A. Sanchez, M. Feld, A. Javan

A low field permanent magnet spin flip Raman laser system[1] has been used to measure the self and foreign gas pressure broadening coefficients of the (000) 5_{15} (010) 6_{24} transition of the ν_2 fundamental vibrational band in water vapor (1884.57 cm^{-1}). In additional we have measured the air broadening of the $\left[(000)\ 5_{32} \rightarrow (010)\ 6_{43}\right]$ transition (1889.58 cm^{-1}).

The experimental arrangement is illustated in Fig. 1. The spin flip Raman laser system consisted of a CO pump laser and an InSb crystal situated in the field of a permanent magnet. The CO laser was a rigid four rod structure with a totally reflecting mirror at one end and a grating mounted in Littrow, used for frequency selection at the other end, both internal to the cavity. The grating coupled out 10% of the radiation inside the laser cavity by means of diffraction into the zeroth order. In order to maintain constant orientation of the output beam while tuning the grating, a reflector was mounted with it in a dihedral configuration.[2] The laser tube was of the three-walled type with a vacuum jacket surrounding the coolant a circulating solution of 2-methylbutane[3] maintained at a temperature of about ∿130°C. The gas flow mixture was similar to that reported by Osgood, et. at.,[4] except that to eliminate impurities the mixture was passed through an activated alumina filter[5] and then through a dry ice-methanol cold trap. Output powers up to 2 watts on a single line were obtained from a laser with 92 cm discharge path.

The spin-flip radiation was generated in an InSb crystal with a carrier concentration of 1×10^{15} cm^{-3} immersed in liquid helium cooled to below the λ point. The CO pump radiation was focused onto the crystal with a 10 cm focal length CaF_2 lens. Spin flip radiation was emitted colinear with the pump beam in both forward and backward directions. The forward output together with the remainder of the pump beam was collected by another 10 cm focal length CaF_2 lens and sent to a Fabry-Perot interferometer.

The backward output was collected by the original focusing lens and was used as the actual spectroscopic source. Use of the same lens for focusing the pump beam and for collecting the spin-flip radiation automatically insured that the backward spin-flip output was colinear with the pump radiation. This allowed us to adjust the lens so that the pump was optimally focused on the crystal without seriously misaligning the spin-flip beam.

In the past it has been difficult to obtain good frequency calibration of the spin-flip laser. (Estimates using the g factor of InSb and measuring the magnetic field can lead to inaccuracies.) In the present experiments the frequency scale was independently established using a Fabry-Perot interferometer with adjustable mirror spacing. The method of coincidences was used to calibrate the frequency tuning of the spin-flip radiation. In this way a frequency scale accurate to a few percent was achieved.

With the polarization of the pump beam parallel to the magnetic field the polarization of the Stokes line of the spin-flip laser is normal to that direction. Therefore, a silicon beam splitter oriented near the Brewster angle was used to reflect most of the backward spin-flip radiation, while transmitting almost all the pump light. The piece of silicon was affixed to a mirror at a dihedral angle of 135° in order to maintain a constant deflection angle of the spinflip beam of 270°, independent of the rotation of the unit. In order to eliminate any residual pump radiation reflected by the beam splitter, the beam was passed through a polarizer consisting of two pieces of germanium placed at Brewster's angle for the spin-flip radiation. A second silicon beam splitter was used to divided the spin-flip radiation into two approximately equal parts. One part was sent through the absorption cell to a detector, while the remainder went directly to another detector. After processing by lock-in amplifiers, these signals were fed into a ratio divider. In this way amplitude variations caused by flucturations in the spin-flip output during frequency tuning were eliminated. Care was also taken to insure that the air paths for the reference beam and the beam sent to the absorption cell were about equal. Thus absorption due to the presence of water vapor in the surrounding air could be balanced out.

The absorption cell was an 80 cm long glass tube with a 5 cm i.d. The CaF_2 windows were mounted at Brewster's angle. For the foreign gas broadening measurements the cell was brought

into equilibrium with the vapor pressure of a water reservoir maintained at 0° C. The reservoir was kept open to the cell during all subsequent additions of foreign gas. This provided a constant 4.6 torr partial pressure of water vapor. After each addition of foreign gas it was found important to wait a sufficient amount of time, usually five minutes, to permit the gases to mix completely and come to equilibrium. For the self-broadening measurements the reservoir was kept at room temperature and we were limited to a maximum water vapor pressure of approximately 20 torr, above which condensation began to take place inside the cell.

The CO laser was made to oscillate on the $P_{9-8}(12)$ line at 1888.32 cm^{-1}. The permanent magnet had tapered pole peices and was mounted on a moveable platform which could be positioned so that the first Stokes line of the spin-flip radiation was at 1884.57 cm^{-1}, using the Fabry-Perot interferometer for calibration. Fine frequency tuning was then done electronically by means of two Helmholtz coils mounted on the permanent magnet. By applying a 1.5 amp current ramp to the coils, we were able to tune through a frequency range of 6.8 GHz. A voltage proportional to the current and therfore to the tuning frequency, was applied to the X-axis of the X-Y recorder. Some typical recordings of foreign gas broadening of water vapor are shown in Fig. 2.

The results of the self and foreign gas broadening measurements are plotted in Fig. 3. Pressures were read using two mechanical Wallace-Tiernan guages, one 0-20 torr and the

other 0-100 torr. The frequency scale was calibrated by means of the Fabry Perot. The results for the pressure broadening coefficients are listed in Table I. The measurements are in good agreement with those predicted by Benedict and Kaplan[6,7] who used Anderson's theory of line broadening[8] to calculate collision broadening coefficients for rotational transitions of the H_2O grand vibrational state. The fact that the microwave predictions agree with our infrared measurements supports the contention[9] that the microwave calculations are also accurate for optical transitions of low J. Pressure shifts for the 1884.57 cm^{-1} line were also observed. In each case the peak of the absorption line shifted to lower frequencies with increasing foreign-gas pressure, but detailed measurements were not taken.

We have also measured the absorption line width of the $[000, 5_{32} - 010, 6_{43}]$ transition of the ν_2 band of water vapor present in the atmosphere 22 C and 35% relative humidity (7 torr).

To avoid excessive absorption by this extremely strong line the air path of the spin-flip beam was reduced to approximately 25 cm. We measured 6.16 $\pm$ 1.0 GHz for the full width at half maximum. Our measured air broadening coefficient is then 8.1 $\pm$ 1.3 MHz/torr, as compared to the theoretically predicted value[6] of 6.11 MHz/torr. Further work on this line is planned for the near future.

Measurements of this type do not require a high degree of frequency stability. Nevertheless, the spin-flip laser

is intrinsically capable of the stability necessary for high-resolution saturation spectroscopy.[10,11,12] However, in our measurements there were indications that at times the spin-flip laser was multimoding. We are currently in the process of eliminating the excess modes and frequency locking the spin-flip laser output to that of a second stabilized CO laser.

In conclusion, we have shown that predictions based on Anderson's theory of collision broadening are valid for low J transitions of water vapor. Discrepancies between theory and experimental results still exist for those transitions of high J,[13,14] and further study is needed before a comprehensive evaluation of the various theoretical models can be made.

We would like to thank Richard Eng for helpful comments during the course of this work.

BIBLIOGRAPHY

1. M. A. Guerra, S. R. Brueck, A. Mooradian, IEEE J. Quant Electron, QE-9, 1157 (1973)
2. T. M. Hard. Appl. Optics Vol. 9 P1825 August 1970.
3. M. M. Mann, M. L. Bhaumik, W. B. Locina, Appl. Phys. Lett, 430 1970.
4. R. M. Osgood, W. E. Eppers, E. R. Nichols, IEEE J. Quant Electron, QE-6, p 145, 1970
5. R. E. Center, IEEE J. Quant. Electron, QE-10 P 208-213 Feb. 1974
6. W. S. Benedict, I. D. Kaplan, J. of Chem. Phys, Vol. 30 pg. 388 Feb 1959
7. W. S. Benedict and L. D. Kaplan JQSRT, Vol. 4 P.453 1964
8. P. W. Anderson, Phys. Rev., vol 76, Pp 647-661
9. W. S. Benedict, op cit p. 396
10. C. K.N. Patel, Phys. Rev. Lett, vol 28, pp. 649-652 March 1972.
11. CKN Patel, App. Phys. Lett vol 25, pp. 112-114 July 1974
12. S. R. Brueck, A. Mooradian, IEEE J. Quant. Electron, QE-10, pp 634-641, Sept 1974
13. R. S. Eng. et al Appl. Phys. Lett, vol 21, pp. 303-305, October 1972.
14. F. A. Blum, et al Science 177, p. 694 1972

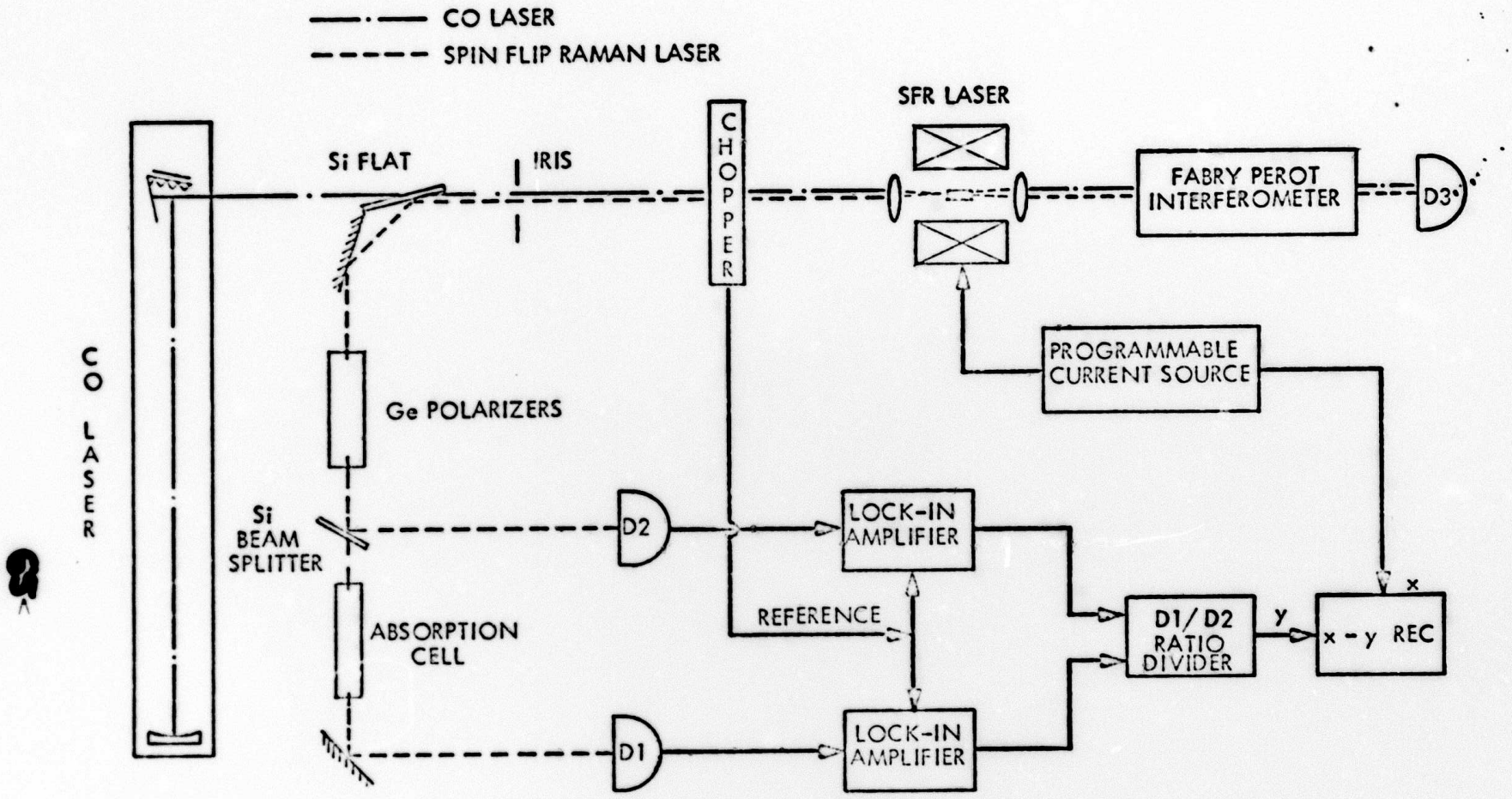
CO LASER
SPIN FLIP RAMAN LASER
SFR LASER
Si FLAT
IRIS
CHOPPER
FABRY PEROT INTERFEROMETER
D3
CO LASER
Ge POLARIZERS
PROGRAMMABLE CURRENT SOURCE
Si BEAM SPLITTER
D2
LOCK-IN AMPLIFIER
REFERENCE
ABSORPTION CELL
D1/D2 RATIO DIVIDER
y
x
x - y REC
D1
LOCK-IN AMPLIFIER

Figure 1

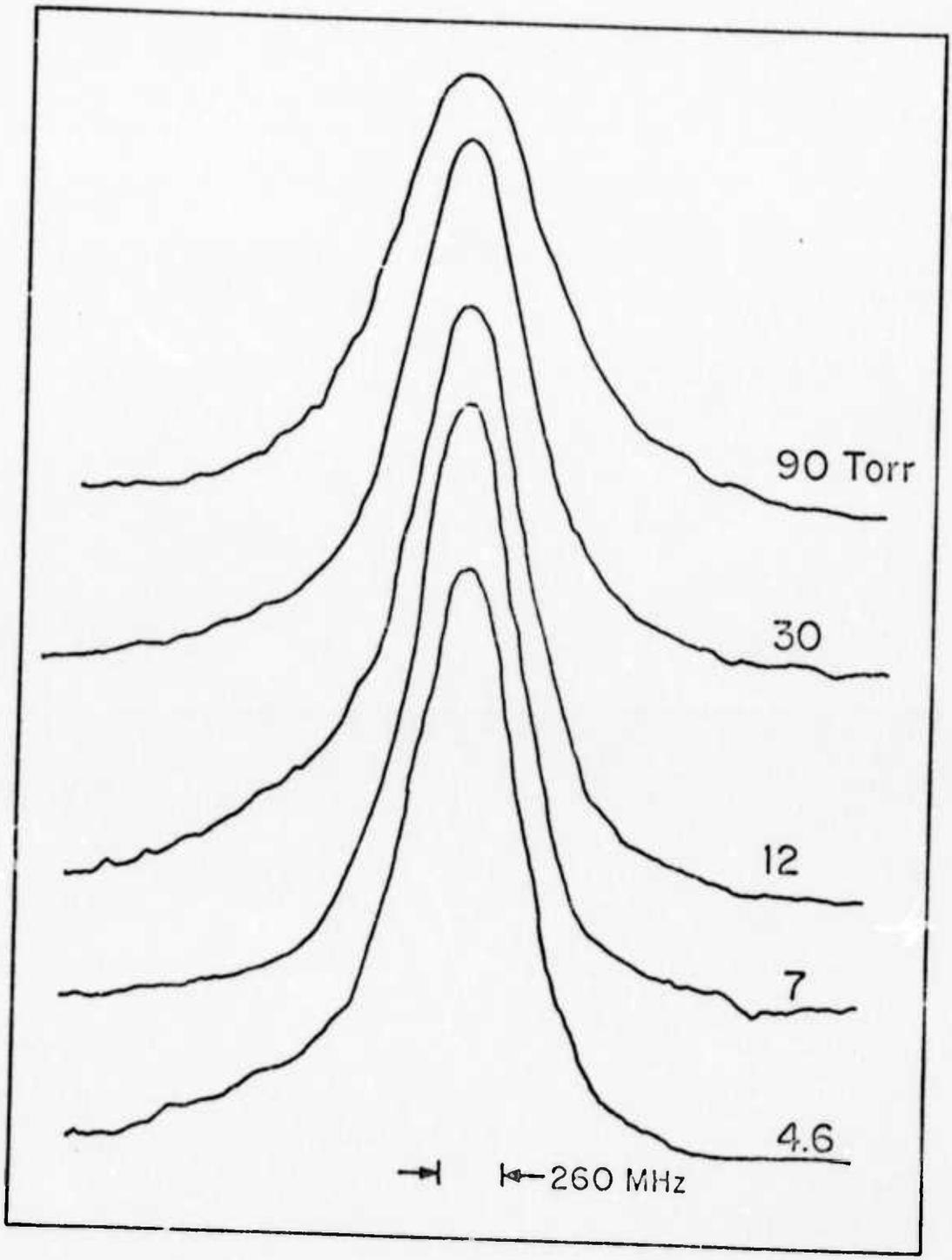

Fig. 2

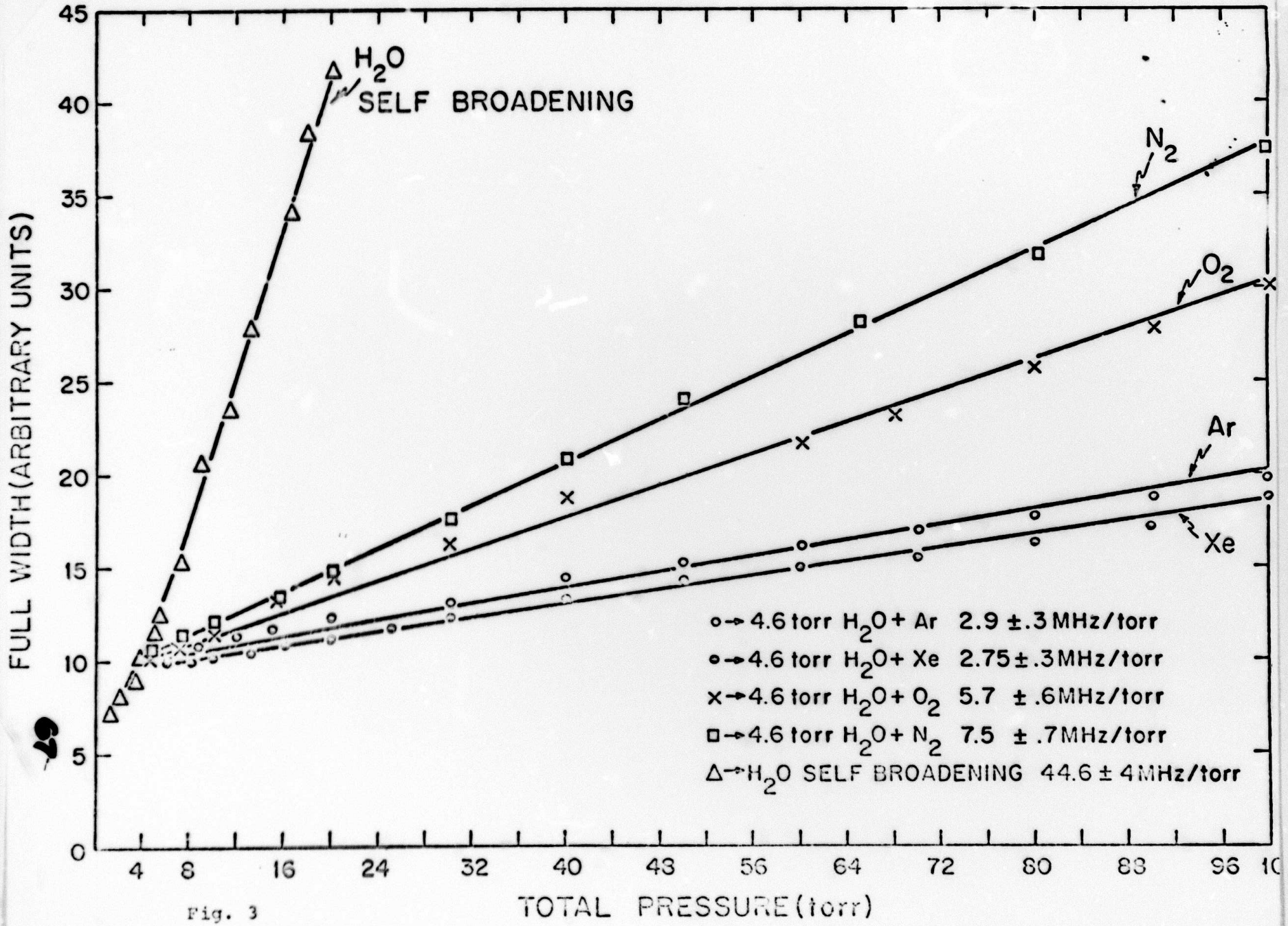
H_2O
SELF BROADENING
N_2
O_2
Ar
Xe
FULL WIDTH (ARBITRARY UNITS)
TOTAL PRESSURE (torr)
0
5
10
15
20
25
30
35
40
45
4
8
16
24
32
40
48
56
64
72
80
88
96
o→ 4.6 torr H_2O + Ar 2.9 ± .3 MHz/torr
o→ 4.6 torr H_2O + Xe 2.75 ± .3 MHz/torr
×→ 4.6 torr H_2O + O_2 5.7 ± .6 MHz/torr
□→ 4.6 torr H_2O + N_2 7.5 ± .7 MHz/torr
△→ H_2O SELF BROADENING 44.6 ± 4 MHz/torr

Fig. 3

	H_2O	N_2	O_2	Ar	Xe
Present Study	44.6±4	7.5±0.7	5.7±0.6	2.9±0.3	2.75±0.2
Theoretical Calculation (1.2)	42.10	7.32	—	—	—

Pressure broadening coefficients of the [000, 5_{15} - 010, 6_{43}] transition of the ν_2 fundamental vibrational band of water vapor.

TABLE 1